Article

Synthesis and Reaction of [{HC(CMeNAr)}Mn] (Ar = 2,6-*i*PrCH): The Complex Containing Three-Coordinate Manganese(I) with a Mn–Mn Bond Exhibiting Unusual Magnetic Properties and Electronic Structure

Jianfang Chai, Hongping Zhu, A. Claudia Stckl, Herbert W. Roesky, Jrg Magull, Alessandro Bencini, Andrea Caneschi, and Dante Gatteschi

J. Am. Chem. Soc., **2005**, 127 (25), 9201-9206• DOI: 10.1021/ja042269e • Publication Date (Web): 01 June 2005

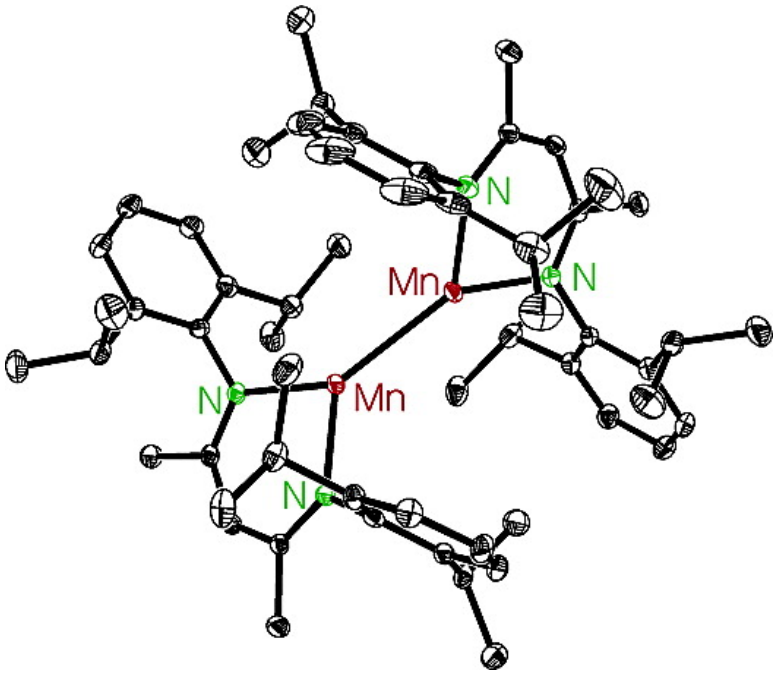

More About This Article

Additional resources and features associated with this article are available within the HTML version:

- Supporting Information
- Links to the 8 articles that cite this article, as of the time of this article download
- Access to high resolution figures
- Links to articles and content related to this article
- Copyright permission to reproduce figures and/or text from this article

Journal of the American Chemical Society is published by the American Chemical Society. 1155 Sixteenth Street N.W., Washington, DC 20036

J|A|C|S
ARTICLES
Published on Web 06/01/2005

Synthesis and Reaction of $[\{HC(CMeNAr)_2\}Mn]_2$ (Ar = 2,6-*i*$Pr_2C_6H_3$): The Complex Containing Three-Coordinate Manganese(I) with a Mn−Mn Bond Exhibiting Unusual Magnetic Properties and Electronic Structure

Jianfang Chai,[†] Hongping Zhu,[†] A. Claudia Stückl,[†] Herbert W. Roesky,*[,†] Jörg Magull,[†] Alessandro Bencini,[‡] Andrea Caneschi,[‡] and Dante Gatteschi[‡]

Contribution from the Institut für Anorganische Chemie der Universität Göttingen, Tammannstrasse 4, D-37077 Göttingen, Germany, and Dipartimento di Chimica and INSTM Research Unit, Polo Scientifico dell'Università di Firenze, via della Lastruccia 3, I-50019, Sesto Fiorentino, Italy

Received December 23, 2004; E-mail: hroesky@gwdg.de

Abstract: This paper reports on the synthesis, X-ray structure, magnetic properties, and DFT calculations of $[\{HC(CMeNAr)_2\}Mn]_2$ (Ar = 2,6-*i*$Pr_2C_6H_3$) (**2**), the first complex with three-coordinate manganese(I). Reduction of the iodide $[\{HC(CMeNAr)_2\}Mn(\mu\text{-I})]_2$ (**1**) with Na/K in toluene afforded **2** as dark-red crystals. The molecule of **2** contains a Mn_2^{2+} core with a Mn−Mn bond. The magnetic investigations show a rare example of a high-spin manganese(I) complex with an antiferromagnetic interaction between the two Mn(I) centers. The DFT calculations indicate a strong s−s interaction of the two Mn(I) ions with the open shell configuration ($3d^54s^1$). This suggests that the magnetic behavior of **2** could be correctly described as the coupling between two $S_1 = S_2 = {}^5/_2$ spin centers. The Mn−Mn bond energy is estimated at 44 kcal mol^{-1} by first principle calculations with the B3LYP functional. The further oxidative reaction of **2** with $KMnO_4$ or O_2 resulted in the formation of manganese(III) oxide $[\{HC(CMeNAr)_2\}Mn(\mu\text{-O})]_2$ (**3**). Compound **3** shows an antiferromagnetic coupling between the two oxo-bridged manganese(III) centers by magnetic measurements.

Introduction

Transition metal complexes containing low-valent and low-coordinate metal centers are rare. This is partly due to the difficulty associated with such metal ions acquiring the stable 16 or 18 valence electrons in the metal orbitals. The employment of sterically hindered organic ligands can somewhat kinetically stabilize transition metal centers in low coordination; however, the reactivity studies of these compounds are not well investigated. Recent publications have shown that the unusual orbital structure of these complexes resulting from the low-coordinate metal centers would render their reactivity very interesting.[1] It has been reported that reduction of the three-coordinate iron(II) chloride $\{HC(CtBuNAr)_2\}FeCl$ (Ar = 2,6-*i*$Pr_2C_6H_3$) leads to the formation of the iron(I) dinitrogen complex $[\{HC(CtBuNAr)_2\}FeN]_2$. Upon further reduction of this compound with potassium, $[K\{HC(CtBuNAr)_2\}FeN]_2$ was obtained containing a $[FeNNFe]^0$ core.[2] Other transition metal compounds with low-valent and low-coordinate metal centers have been synthesized, for example, for Co, Ni, and Cu,[1,3] and the reactivity studies of Cu(I) compounds are notable.[4] Complexes with manganese(I) (or lower oxidation states) are known to be important due to their participation in photochemistry.[5] In the course of our investigation, the great majority of manganese(I) (and lower oxidation states) complexes are reported for carbonyl compounds. Complexes with low-valent manganese incorporating noncarbonyl ligands are not abundant,[6] although the chemistry of these species is quite interesting.[7] Correspondingly, a few complexes with three-coordinate, even two-coordinate, manganese centers are known; however, these compounds have oxidation states of +2 or higher in metal centers.[8] In this regard,

[†] Universität Göttingen.
[‡] Università di Firenze.

(1) Holland, P. L.; Cundari, T. R.; Perez, L. L.; Eckert, N. A.; Lachicotte, R. J. *J. Am. Chem. Soc.* **2002**, *124*, 14416−14424.
(2) Smith, J. M.; Lachicotte, R. J.; Pittard, K. A.; Cundari, T. R.; Lukat-Rodgers, G.; Rodgers, K. R.; Holland, P. L. *J. Am. Chem. Soc.* **2001**, *123*, 9222−9223.
(3) (a) Holland, P. L.; Tolman, W. B. *J. Am. Chem. Soc.* **1999**, *121*, 7270−7271. (b) Holland, P. L.; Tolman, W. B. *J. Am. Chem. Soc.* **2000**, *122*, 6331−6332. (c) Randall, D. W.; George, S. D.; Holland, P. L.; Hedman, B.; Hodgson, K. O.; Tolman, W. B.; Solomon, E. I. *J. Am. Chem. Soc.* **2000**, *122*, 11632−11642. (d) Jazdzewski, B. A.; Holland, P. L.; Pink, M.; Young, V. G., Jr.; Spencer, D. J. E.; Tolman, W. B. *Inorg. Chem.* **2001**, *40*, 6097−6107.
(4) (a) Spencer, D. J. E.; Aboelella, N. W.; Reynolds, A. M.; Holland, P. L.; Tolman, W. B. *J. Am. Chem. Soc.* **2002**, *124*, 2108−2109. (b) Aboelella, N. W.; Lewis, E. A.; Reynolds, A. M.; Brennessel, W. W.; Cramer, C. J.; Tolman, W. B. *J. Am. Chem. Soc.* **2002**, *124*, 10660−10661. (c) Aboelella, N. W.; Kryatov, S. V.; Gherman, B. F.; Brennessel, W. W.; Young, V. G., Jr.; Sarangi, R.; Rybak-Akimova, E. V.; Hodgson, K. O.; Halman, B.; Soloman, E. I.; Cramer, C. J.; Tolman, W. B. *J. Am. Chem. Soc.* **2004**, *126*, 16896−16911. (d) Lewis, E. A.; Tolman, W. B. *Chem. Rev.* **2004**, *104*, 1047−1076.
(5) Roundhill, D. M. *Photochemistry and Photophysics of Metal Complexes*; Plenum Press: New York, 1994.
(6) (a) Reardon, D.; Aharonian, G.; Gambarotta, S.; Yap, G. P. A. *Organometallics* **2002**, *21*, 786−788. (b) Gibson, V. C.; Segal, J. A.; White, A. J. P.; Williams, D. J. *J. Am. Chem. Soc.* **2000**, *122*, 7120−7121. (c) Bourget-Merle, L.; Lappert, M. F.; Severn, J. R. *Chem. Rev.* **2002**, *102*, 3031−3066.

Scheme 1. Preparation of Compound **2**

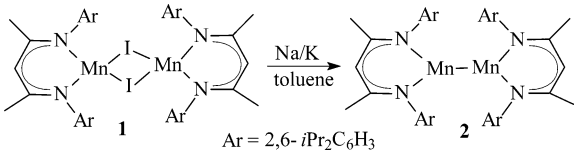

following the recent success that low-valent and/or low-coordinate metal centers are stabilized by the sterically bulky β-diketiminato ligands, it is of great interest to assemble complexes with low-valent and low-coordinate manganese by using such ligands and, meanwhile, to explore their reactivity. Herein, we report on the synthesis and X-ray structure of [{HC(CMeNAr)$_2$}Mn]$_2$ (**2**), the first example of a three-coordinate manganese(I) compound. The magnetic properties and electronic structure (by DFT calculations) of **2** are also investigated, as well as its oxidative reaction to manganese(III) oxide [{HC(CMeNAr)$_2$}Mn(μ-O)]$_2$ (**3**).

Results and Discussion

Synthesis, Structure, and Reaction. The reduction of the bis(μ-iodo)dimanganese(II) complex [{HC(CMeNAr)$_2$}Mn(μ-I)]$_2$ (**1**)[9] with a Na/K alloy in toluene at room temperature affords [{HC(CMeNAr)$_2$}Mn]$_2$ (**2**) as dark-red crystals in about 15% yield. Compound **2** is highly air-sensitive, and decomposition occurs, even when it is kept in solid state at argon atmosphere. It is thermally stable and melts at 154−156 °C. The most intense peak in the EI mass spectrum of **2** appeared at *m*/*z* 472, corresponding to half of the molecule. The signal at *m*/*z* 944 (5%) was assigned to the molecular ion [M$^+$]. Single crystals of **2** suitable for X-ray structural analysis were obtained by keeping the toluene solution of **2** at 4 °C for 1 week. Crystallographic data are given in Table 1 and selected bond lengths and angles in Table 2. The molecular structure of **2** reveals a dimer containing a central Mn_2^{2+} core with a Mn−Mn bond (Figure 1). Each Mn atom is three-coordinate by two N atoms of the L ligand and one adjacent Mn atom. The sum of the bond angles around each Mn averages to 359.4°, indicating the trigonal planar coordination geometry of the respective manganese center. The two Mn−Mn atoms are each terminally chelated by L ligands, forming two six-membered C_3N_2Mn rings in approximately an orthogonal array (dihedral angle, 80.6°). In the C_3N_2Mn ring, the C_3N_2 part is planar and a Mn atom is significantly out of this plane (av 0.53 Å). The Mn−N bond lengths (av 2.10 Å) are slightly longer than those observed in **1** (av 2.07 Å), and the N−Mn−N angle (89.82°) in **2** is more acute than that in **1** (av 94.59°).[9] The Mn−Mn bond length in **2** (2.72 Å) is significantly shorter than that in the Mn(0) compound $Mn_2(CO)_{10}$ (2.90 Å)[10] and can be compared with that in the Mn(I) complex $Mn_2(CO)_7(\mu\text{-}S_2)$ (2.67 Å),[11] whereas similar Mn−Mn separations are found in the alkyl-bridged Mn(II) compounds [(PhCMe$_2$CH$_2$)Mn(μ-CH$_2$-CMe$_2$Ph)]$_2$ (2.72 Å)[12] and [{HC(CMeNAr)$_2$}Mn(μ-Me)]$_2$ (2.81 Å).[3b] However, these Mn−Mn bond distances are shorter than those observed for the "naked" Mn_2 (3.4 Å) and Mn_2^{2+} (3.06 Å) species.[14]

In view of the rich chemistry of low-valent Mn−Mn complexes, such as $Mn_2(CO)_{10}$ and $Mn_2(CO)_7(\mu\text{-}S_2)$,[10,11] it is of great interest to explore the reactivity of **2**. Here, we examined

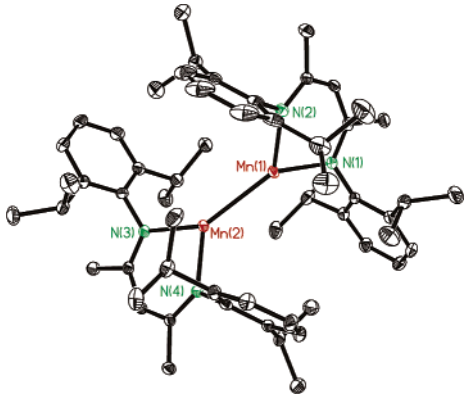

Figure 1. ORTEP drawing for complex **2** (30% probability ellipsoids).

Table 1. Crystallographic Data for Complexes **2** and **3**

	2	**3**
formula	$C_{58}H_{82}Mn_2N_4$	$C_{58}H_{82}Mn_2N_4O_2$
Fw	945.16	977.16
T (K)	133(2)	133(2)
cryst. syst.	monoclinic	monoclinic
space group	$P2(1)/c$	$C2/c$
a (Å)	14.4602(9)	15.4921(12)
b (Å)	14.2263(6)	16.3958(9)
c (Å)	26.795(2)	21.3688(17)
β (°)	94.999(6)	90.802(6)
V (Å^3)	5491.1(6)	5427.3(7)
Z	4	4
d_{calcd} (g cm^{-3})	1.143	1.196
μ (mm^{-1})	0.498	0.509
F(000)	2032	2096
2θ range (°)	3.24 to 49.62	3.62 to 49.54
No. of rflns collected	38085	18243
No. of ind rflns	9401 (R(int) = 0.1276)	4641 (R(int) = 0.0637)
No. of data/restraints/params	9401/0/597	4641/0/308
goodness of fit, F^2	0.953	1.024
$R1$, $wR2$ [$I > 2\sigma(I)$]	0.0414, 0.0781	0.0421, 0.0873
$R1$, $wR2$ (all data)	0.0716, 0.0825	0.0664, 0.0962
largest diff peak (e Å^{-3})	0.496 to −0.567	0.325 to −0.257

Table 2. Selected Bond Lengths (Å) and Bond Angles (°) for Compounds **2** and **3**

	Compound **2**		
Mn(1)−N(1)	2.097(2)	N(1)−Mn(1)−N(2)	89.72(9)
Mn(1)−N(2)	2.101(2)	N(1)−Mn(1)−Mn(2)	139.96(6)
Mn(1)−Mn(2)	2.721(1)	N(2)−Mn(1)−Mn(2)	129.67(6)
Mn(2)−N(3)	2.116(2)	N(3)−Mn(2)−N(4)	89.92(8)
Mn(2)−N(4)	2.094(2)	N(3)−Mn(2)−Mn(1)	141.26(6)
	Compound **3**		
Mn(1)−N(1)	2.013(2)	N(1)−Mn(1)−N(2)	90.28(8)
Mn(1)−N(2)	2.013(2)	N(1)−Mn(1)−O(1)	96.64(8)
Mn(1)−O(1)	1.809(2)	N(2)−Mn(1)−O(1)	157.90(9)
Mn(1)−O(1A)	1.827(2)	O(1)−Mn(1)−O(1A)	85.99(7)
Mn(1)−Mn(1A)	2.659(1)	N(1)−Mn(1)−O(1A)	156.26(8)

(7) Treichel, P. M. In *Comprehensive Organometallic Chemistry*; Wilkinson, G., Stone, F. G. A., Abel, E. W., Eds.; Elsevier: Oxford, UK, 1982.
(8) (a) Ellison, J. J.; Power, P. P.; Shoner, S. C. *J. Am. Chem. Soc.* **1989**, *111*, 8044−8046. (b) Wehmschulte, R. J.; Power, P. P. *Organometallics* **1995**, *14*, 3264−3267. (c) Panda, A.; Stender, M.; Wright, R. J.; Olmstead, M. M.; Klavins, P.; Power, P. P. *Inorg. Chem.* **2002**, *41*, 3909−3916. (d) Chai, J.; Zhu, H.; Fan, H.; Roesky, H. W.; Magull, J. *Organometallics* **2004**, *23*, 1177−1179.
(9) Chai, J.; Zhu, H.; Most, K.; Roesky, H. W.; Vidovic, D.; Schmidt, H.-G.; Noltemeyer, M. *Eur. J. Inorg. Chem.* **2003**, 4332−4337.
(10) Bianchi, R.; Gervasio, G.; Marabello, D. *Inorg. Chem.* **2000**, *39*, 2360−2366 and references therein.
(11) (a) Adams, R. D.; Kwon, O.-S.; Smith, M. D. *Inorg. Chem.* **2001**, *40*, 5322−5323. (b) Adams, R. D.; Kwon, O.-S.; Smith, M. D. *Inorg. Chem.* **2002**, *41*, 5525−5529.
(12) Andersen, R. A.; Carmona-Guzman, E.; Gibson, J. F.; Wilkinson, G. *J. Chem. Soc., Dalton Trans.* **1976**, 2204−2211.

Scheme 2. Formation of **3** by Oxidation of **2**

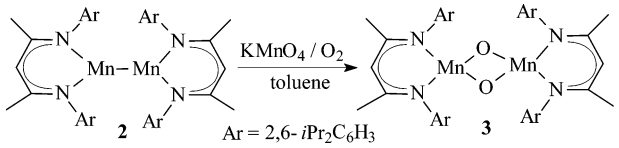

its reactivity toward the oxidative reagents $KMnO_4$ and molecular O_2 in an attempt to approach manganese oxides, which are believed to be involved in many natural processes such as water oxidation and O_2 evolution by means of the photosystem II.[14] After stirring a mixture of **2** and excess $KMnO_4$ in toluene at room temperature for 2 days, a dimeric manganese oxide [{HC(CMeNAr)$_2$}Mn(μ-O)]$_2$ (**3**) was smoothly afforded as red crystals in high yield. The alternative reaction of **2** with predried dioxygen gave the same result. Compound **3** is thermally stable. It melts at 213−215 °C, and the EI-MS spectrum gives the most intense peak at *m*/*z* 976 for the molecular ion of **3**.The molecular structure of **3** is shown in Figure 2. Crystallographic data and selected bond lengths and angles are given in Tables 1 and 2, respectively. This compound contains two peripheral six-membered C_3N_2Mn rings and one central four-membered Mn_2O_2 ring. The dihedral angle between the six- and the four-membered rings is 39.9°. Each manganese center is tetrahedrally coordinated. The Mn−N distances (av 2.01 Å) are a slightly shorter than those in **2**, while the N−Mn−N angle (90.28(8)°) is close to that in **2**. The Mn−O distances in **3** average to 1.82 Å and fall in the normal range (1.79−1.86 Å).[15] The Mn−Mn distance in **3** is 2.66 Å and is the shortest separation among those bis(μ-oxo)dimanganese(III) centers. It is a little shorter compared to that in **2**, indicating considerable contacts within the Mn_2O_2 core.

Magnetic Properties and Electronic Structure of 2. The temperature dependence of the magnetic susceptibility of **2** in the temperature range of 2−290 K is shown in Figure 3. The room temperature effective magnetic moment (μ_{eff} = 3.93 μ_B) suggests that the manganese(I) ions are in a high spin state derived either from the free ion ($3d^54s^1$) configuration, ^{7}S, or from the $3d^6$ electronic configuration, ^{5}D. However, it is much smaller than that expected for two noninteracting manganese(I) centers, μ_{eff} = 9.8 μ_B for ^{7}S and μ_{eff} = 6.9 μ_B for ^{5}D states, respectively. This may indicate that an antiferromagnetic interaction between the metal centers with Curie temperature (T_C) higher than 300 K is operative, as confirmed by the fact that χ smoothly decreases in the temperature range from 300 to 20 K without going through a maximum. Below 10 K, the χ increases versus *T*, again, indicating the presence of a small paramagnetic impurity. As a matter of fact, **2** was found to be highly air-sensitive, and although particular care was taken in the preparation of the sample, some decomposition was likely to occur. In the temperature range of 10−20 K, the χ versus *T* curve reaches a minimum significantly different from zero. This implies that a sizable temperature-independent paramagnetism is present together with some paramagnetic impurity. EPR spectra recorded with freshly filtered single crystals at 9.4 and 95 GHz, respectively, showed a number of signals disappearing at temperatures lower than 10 K (Figures S2a and S2b, in the Supporting Information) and are indicative of an antiferromagnetic behavior, contrary to the ferromagnetism observed for Mn_2^{2+} isolated in rare gas matrixes.[17]

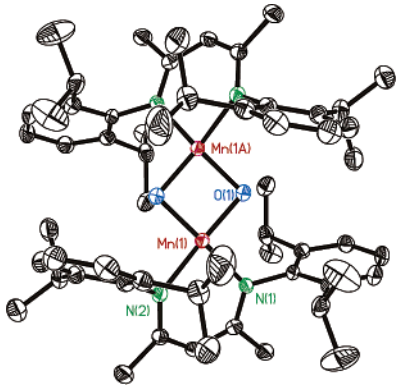

Figure 2. ORTEP drawing for complex **3** (50% probability ellipsoids).

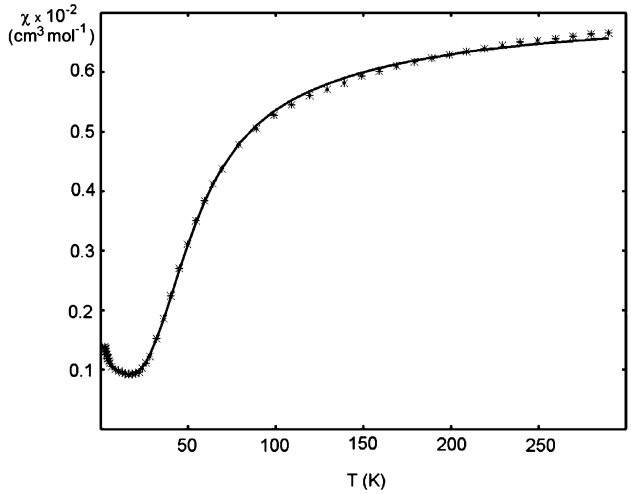

Figure 3. Temperature dependence of the magnetic susceptibility of **2**.

Direct information for the value of the spins S_i of the manganese(I) ions in **2** cannot be obtained since we are not able to measure susceptibility values at temperatures higher than T_C. However, it is worth mentioning that the χ versus *T* curve could be reproduced with any value of $3 \geq S_i \geq 2$, as shown by the calculations. The magnetic data alone are not sufficient enough to unambiguously determine the exact spin of the interacting centers; therefore, quantum chemical calculations of the electronic structure of **2** using density functional theory (DFT)[18] were performed as described in the Experimental Section.

It is well-known that the calculation of the magnetic structure of polynuclear transition metal complexes is a delicate quantum chemical problem challenging computational and theoretical chemists for many years.[19] This is because the computed energies fall in the range of *kT* and are, therefore, strongly influenced by small effects, such as the electron correlation.

(13) Selected samples: (a) Seder, T. A.; Church, S. P.; Weitz, E. *J. Am. Chem. Soc.* **1986**, *108*, 1084−1086. (b) Seder, T. A.; Church, S. P.; Weitz, E. *J. Am. Chem. Soc.* **1986**, *108*, 7518−7524.
(14) Nayak, S. K.; Rao, B. K.; Jena, P. *J. Phys.: Condens. Matter* **1998**, *10*, 10863−10878.
(15) (a) Hoganson, C. W.; Babcock, G. T. *Science* **1997**, *277*, 1953−1956. (b) Stubbe, J.; van der Donk, W. A. *Chem. Rev.* **1998**, *98*, 705−762 and references therein.
(16) (a) Kitajima, N.; Singh, U. P.; Amagai, H.; Osawa, M.; Morooka, Y. *J. Am. Chem. Soc.* **1991**, *113*, 7757−7758. (b) Goodson, P. A.; Oki, A. R.; Glerup, J.; Hodgson, D. J. *J. Am. Chem. Soc.* **1990**, *112*, 6248−6254. (c) Goodson, P. A.; Hodgson, D. J. *Inorg. Chem.* **1989**, *28*, 3606−3608.
(17) Van Zee, R. J.; Weltner, W., Jr. *J. Chem. Phys.* **1988**, *89*, 4444−4446.
(18) *Reviews of Modern Quantum Chemistry*; Sen, K. D., Ed.; World Scientific: Singapore, 2002.

The description of the lowest spin state of the systems, in particular, requires the use of open-shell multiconfigurational wave functions that can be correctly handled only with multireference configuration interaction approaches.[20] These approaches become, however, unusable for large molecular systems, due to the extremely large number of configurations required, and formalisms have been developed to approximately include these effects into DFT,[21] which is a single determinant-based theory. These efforts result in DFT being the most widely used tool for the interpretation of magnetic properties due to its high accuracy/CPU cost ratio. The use of the B3LYP functional and the broken symmetry formalism was found to provide results that are generally, at least, in semiquantitative agreement with the experimental data. Furthermore, the magnetic behavior of molecules is strongly influenced by modelization of the chemical systems,[22] which is unavoidable in multiconfigurational calculations in order to reach a reasonable computational time. Again, within DFT, it is possible to use the real chemical system in the calculations of the magnetic coupling constants.

Single-point calculations were performed using the molecular coordination obtained by the X-ray single-crystal structure to compute the magnetic exchange coupling constant (J) and to characterize the bonding interactions. The Heisenberg−Dirac−vanVleck spin Hamiltonian in the form $H = J(\boldsymbol{S_1 \cdot S_2})$ was used, with a positive J value determining a singlet ground state. The magnetic exchange coupling constant was computed by using the broken symmetry (BS) approach.[19] The BS calculations were performed imposing mirror symmetry to the α and β electrons on the two Mn atoms, and the resulting wave function has, therefore, $M_S = 0$. Due to the mirror symmetry imposed on the spin densities, the BS molecular orbital can be spatially localized onto different parts of the molecule and is assumed to be a good description of the natural magnetic orbitals, with the extent of the localization depending on the overlap between the orbitals.[19d] In the SOMO region, the BS wave function of **2** is characterized by a series of occupied 3d spin−orbitals almost centered onto the manganese atoms and rather well localized on the two different halves of the molecule according to their α/β occupancy (α orbitals being localized on the Mn(1) atom). The HOMO, on the contrary, which lies above the SOMO's, is delocalized onto the two metal centers, as shown in Figure 4. The α and β components have almost the same spatial extent, which shows the formation of a metal−metal σ bond. The Mulliken population analysis assigns a spin population (spin density) of 4.9 to each Mn center. Transforming the computed molecular orbitals into natural bond orbitals (NBO)[23,24] allowed a natural population analysis (NPA) that assigned to each manganese center the electronic configuration ($4s^{1.02}3d^{5.14}4p^{0.01}$) with a natural charge of 0.83, in agreement with the formal oxidation state (+1) of the manganese ion. The natural spin densities are 4.91, with opposite sign on each manganese atom. The Mn−Mn NBOs are computed for α and β spins with 0.96 occupancy. Their composition is shown in Table 3. The Mn−Mn bond is, therefore, mainly formed by the 4s orbitals of the manganese atoms with a small contribution of 3d electrons. A crude estimate of the Mn−Mn bonding energy can be obtained by subtracting from the total energy of the molecule those of the fragments. This procedure gave a bonding energy of 44 kcal mol^{-1} (B3LYP), which can compare with that calculated for $Mn_2(CO)_{10}$ (38 or 35 kcal mol^{-1})[25] and is much lower than that found for the H_2 molecule (104 kcal mol^{-1}).[26] The binding energies computed for Mn_2 (82 kcal mol^{-1}) and Mn_2^{2+} (70 kcal mol^{-1}) are also larger than that computed for **2**.

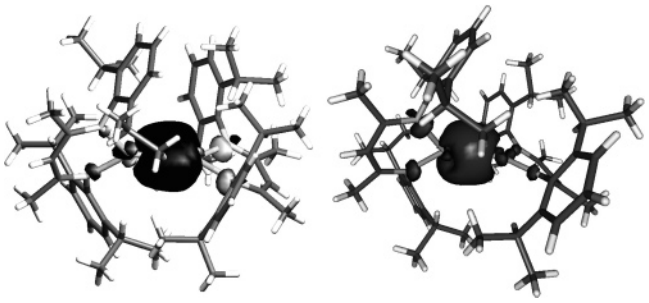

Figure 4. The s bond orbital of **2** (left: the α spin orbital; right: the β spin orbital).

Table 3. The Mn−Mn Natural Bond Orbitals

spin	occupancy	%	Mn(1)	%	Mn(2)
α	0.965	56.5	$4s^{0.96}4p^{0.03}3d^{0.04}$	43.5	$4s^{0.90}4p^{0.02}3d^{0.10}$
β	0.965	43.6	$4s^{0.91}4p^{0.02}3d^{0.09}$	56.4	$4s^{0.96}4p^{0.03}3d^{0.04}$

The above description of the electronic structure of **2** suggests that its magnetic behavior could be properly described as the coupling between two $S_1 = S_2 = {}^5/_2$ spin centers, and the 4s electrons are involved in forming a metal−metal single bond. The magnetic electrons are mainly localized in the metal 3d atomic orbitals. This result could not be easily anticipated from simple considerations based on the electronic structure of the free manganese(I) ion, as usually done for rationalizing the magnetic behavior of transition metal dimers,[25] due to the "quenching" of the magnetic contribution of the 4s electrons when the Mn−Mn bond is formed. The exchange coupling constant (J) can thus be conveniently computed from the energy difference between the $S = 10$ high spin state and the BS state as 110 and 160 cm^{-1} using the B3LYP and BP functionals, respectively.

The best fitting of the magnetic data of **2** was obtained with the procedure described in the Experimental Section. The presence of some $S = {}^5/_2$ paramagnetic impurity was considered in order to reproduce the low-temperature tail of the χ versus T

(19) (a) Noodleman, L.; Norman, J. G., Jr. *J. Chem. Phys*. **1979**, *70*, 4903−4906. (b) Noodleman, L. *J. Chem. Phys.* **1981**, *74*, 5737−5743. (c) Noodleman, L.; Davidson, E. R. *Chem. Phys.* **1986**, *109*, 131−143. (d) Ciofini, I.; Daul, C. A.; Bencini, A. Modeling Molecular Magnetism. In *Recent Advances in DFT Methods*; Barone, V., Bencini, A., Fantucci, P., Eds.; World Scientific: Singapore, 2002.
(20) Miralles, J.; Castell, O.; Caballol, R.; Malrieu, J. P. *Chem. Phys.* **1993**, *172*, 33.
(21) Illas, F.; Moreira, I.; De, P. R.; de Graaf, C.; Barone, V. *Theor. Chem. Acc.* **2000**, *104*, 265.
(22) Adamo, C.; Barone, V.; Bencini, A.; Totti, F.; Ciofini, I. *Inorg. Chem.* **1999**, *38*, 1996−2004.
(23) Reed, A. E.; Curtiss, L. A.; Weinhold, F. *Chem. Rev.* **1988**, *88*, 899−926.
(24) We mention here that the description of bond properties and other molecular properties based on MO pictures and population analysis is subject to several limitations due to the arbitrariness in the choice of the basis functions and of the scheme for partitioning the electronic density in atomic regions. For a critical comparison of some population analyses, one can refer to: Guerra, C. F.; Handgraaf, J.-W.; Baerends, E. J.; Bickelhaupt, F. M. *J. Comput. Chem*. **2003**, *25*, 189−210. It must also be stressed that population analysis is currently used in interpreting polarized neutron diffraction experiments with *semi*quantitative agreement with the experimental data (see for example: Gillon, B.; Mathoniere, C.; Ruiz, E.; Alvarez, S.; Cousson, A.; Rajendiran, T. M.; Kahn, O. *J. Am. Chem. Soc*. **2002**, *124*, 14433−14441.
(25) Rosa, A.; Ehlers, A.; Baerends, E. J.; Snijders, J. G.; te Velde, G. *J. Phys. Chem.* **1996**, *100*, 5690−5696.
(26) Cotton, F. A.; Wilkinson, G. *Advanced Inorganic Chemistry*, 5th ed.; John Wiley & Sons Inc.: New York, 1988.

curve. The best fitting parameters are $J = 109.8(2)$ and $\rho = 0.031(4)\%$ (ρ being the percentage of paramagnetic impurity assumed to have a spin $S = S_1$). The Zeeman g factor and the temperature-independent paramagnetism were kept constant at $g = 2.00$ and TIP $= 830 \times 10^{-6}$ cm^3 mol^{-1}.[27] The agreement factor R ($R = \sum_i|\chi_i^\circ - \chi_i^c|/\sum_i\chi_i^\circ$) was 0.88%. The computed J value is in good agreement with the experimental one, and with the B3LYP results in better quantitative agreement as often found in the literature. Equivalent fits of the magnetic data were obtained for $S_1 = S_2 = 3$ ($J = 109.9(2)$, $\rho = 0.023(4)\%$, TIP $= 830 \times 10^{-6}$ cm^3 mol^{-1}, $R = 0.88\%$) and $S_1 = S_2 = 2$ ($J = 109.7(2)$, $\rho = 0.045(4)\%$, TIP $= 830 \times 10^{-6}$ cm^3 mol^{-1}, $R = 0.95\%$).

Magnetic Measurement of 3. The magnetic data of **3** were recorded in the temperature range of 4−300 K. The magnetic behavior is indicative of an antiferromagnetic coupling between the two manganese(III) centers, $S_1 = S_2 = 2$ in a pseudo-tetrahedral chromophore, mediated by the two oxo-bridges. The μ_{eff} (4.7 μ_B) at room temperature is much lower than the spin-only value expected for two noninteracting $S = 2$ spins ($\mu_{eff} = 6.9\ \mu_B$). The μ_{eff} steadily decreases to $\sim 0\ \mu_B$ at about 24 K (Figure S1). This behavior is consistent with the geometry and the type of bridging atoms. The temperature dependence of the magnetic susceptibility was fitted as described in the Experimental Section. The best fit values are $J = 91.5(5)$, $g = 1.99(2)$, and $R = 0.98\%$.

Conclusions

In summary, we have prepared [{HC(CMeNAr)$_2$}Mn]$_2$ (Ar = 2,6-*i*Pr$_2$C$_6$H$_3$) (**2**), the first complex with three-coordinate manganese(I), by the Na/K alloy reduction of [{HC(CMeNAr)$_2$}Mn(μ-I)]$_2$ (**1**). Compound **2** has a Mn_2^{2+} core with a Mn−Mn bond. The reaction of **2** with $KMnO_4$ or O_2 affords a Mn_2O_2 core compound [{HC(CMeNAr)$_2$}Mn(μ-O)]$_2$ (**3**). The latter oxidation with O_2 of the two Mn(I) centers involves a homolytic cleavage of the Mn−Mn bond, indicating the interesting reactivity of **2** for further investigations.

Experimental Section

General Considerations. All reactions were performed using standard Schlenk and drybox techniques. Solvents were appropriately dried and distilled under dinitrogen prior to use. Elemental analyses were performed by the Analytisches Labor des Instituts für Anorganische Chemie der Universität Göttingen. Mass spectra were obtained on a Finnigan Mat 8230. IR spectra were recorded on a Bio-Rad Digilab FTS-7 spectrometer as Nujol mulls between KBr plates. Magnetic measurements were performed by using a Cryogenic S600 SQUID magnetometer operating with an applied field of 1 Torr. The sample was prepared in a glovebox by grinding freshly filtered crystals. The powder was wrapped in a Teflon tape placed in a special sample holder and placed inside the SQUID without any contact with air. Magnetic susceptibilities were corrected for diamagnetism by using Pascal's constants. [{HC(CMeNAr)$_2$}Mn(μ-I)]$_2$ (**1**) was synthesized as previously reported in the literature.[9]

[{HC(CMeNAr)$_2$}Mn]$_2$ (2). At room temperature, a suspension of **1** (0.60 g, 0.5 mmol) in toluene (30 mL) was added to a Na/K alloy (Na 0.01 g, 0.5 mmol; K 0.04 g, 1 mmol). The mixture was stirred at room temperature for 4 days, and a red solution was obtained. After filtration, the solution was concentrated to ca. 10 mL. Dark-red crystals were obtained after 1 week at 4 °C. Yield: 0.07 g, 15%. Mp 154−156 °C. Anal. Calcd for $C_{58}H_{82}Mn_2N_4$ (945.16): C, 73.65; H, 8.68; N, 5.93. Found: C, 73.62; H, 8.67; N, 5.74. EI-MS: *m*/*z* (%) 944 (5) $[M]^+$, 472 (100) $[1/2M]^+$. IR (KBr, Nujol mull, cm^{-1}): $\tilde{\nu}$ 1698 (w), 1654 (w), 1624 (w), 1577 (w), 1555 (w), 1261 (s), 1092 (s), 1019 (s), 937 (w), 866 (w), 799 (s), 762 (w), 722 (w), 667 (w), 614 (w), 568 (w).

[{HC(CMeNAr)$_2$}Mn(μ-O)]$_2$ (3). Route a: $KMnO_4$ (0.5 g, 3.2 mmol) was added to a solution of **2** (0.2 g, 0.2 mmol) in toluene (20 mL) at room temperature. The mixture was stirred at room temperature for 2 days. Unreacted $KMnO_4$ was removed by filtration. The solvent was removed in vacuum, and the residue was extracted with diethyl ether. Red crystals were obtained after 4 days at 4 °C. Yield: 0.14 g, 72%. Mp 213−215 °C. Anal. Calcd for $C_{58}H_{82}Mn_2N_4O_2$ (977.16): C, 71.23; H, 5.94; N, 5.73. Found: C, 70.92; H, 5.67; N, 5.54. EI-MS: *m*/*z* (%) 976 (100) $[M]^+$. IR (KBr, Nujol mull, cm^{-1}): $\tilde{\nu}$ 1659 (w), 1623 (w), 1592 (w), 1552 (w), 1528 (w), 1261 (s), 1094 (s), 1025 (s), 936 (w), 919 (w), 842 (w), 801 (s), 761 (w), 720 (w), 699 (w), 668 (w), 607 (w), 514 (w), 467 (w). **Route b:** Dry O_2 was introduced into a solution of **2** (0.2 g, 0.2 mmol) in toluene (20 mL) at −78 °C instead of N_2. The solution was kept at this temperature for 2 h and slowly warmed to room temperature and stirred for 12 h. All volatiles were removed in vacuum, and the residue was extracted with diethyl ether. Red crystals were obtained after 7 days at 4 °C. Yield: 0.12 g, 63%.

X-ray Crystallography. Crystallographic data of complexes **2** and **3** were collected on a Stoe IPDS II-array detector system with graphite-monochromated Mo Kα radiation ($\lambda = 0.71073$ Å). The structures were solved by direct methods (SHELXS-97) and refined against F^2 using SHELXL-97.[28] All non-hydrogen atoms were located by difference Fourier synthesis and refined anisotropically. The hydrogen atoms were included at geometrically calculated positions and refined using a riding model.

Computational Details. All of the calculations were performed in the framework of the density functional theory (DFT) with the NWChem4.6.[29] Single-point calculations of the experimental X-ray structure were performed using the B3LYP functional.[30] Calculations with the Becke−Perdew (BP) functional[31,32] were also done for comparison. All electron double-ζ basis set proposed by Ahlrichs was applied to all of the atoms except for Mn, which was treated with the Ahlrichs triple-ζ basis set.[33]

Population analysis based on natural atomic orbitals (NAO) and natural bond orbitals (NBO)[23] was performed using the NBO 5.0 program[34] implemented in NWChem.

Calculations of the exchange coupling constant were performed using the broken symmetry formalism[19] with the working equation, $J = {}^2/_{25}[E(\mathrm{HS}) - E(\mathrm{BS})]$, where E(HS) and E(BS) are the SCF energies of the high spin ($S = 5$) and broken symmetry ($M_S = 0$) states, respectively. The χ versus T curve was fitted using the standard procedure[35] by minimizing the squares' sum of the differences between computed and measured molar susceptibilities with the MINUIT program package.[36] The best fit values are reported in the text.

(27) Due to the high variance−covariance between ρ and TIP (0.87), we performed a series of calculations for various values of TIP between 600×10^{-6} and 900×10^{-6} cm^3 mol^{-1}. The value shown in the text gave the better agreement.

(28) (a) Sheldrick, G. M. *Acta Crystallogr. A* **1990**, *46*, 467−473. (b) Sheldrick, G. M. *SHELXL-97, Program for Crystal Structure Refinement*; Universität Göttingen: Göttingen, Germany, 1997.
(29) High-performance computational chemistry group, *NWChem: A Computational Chemistry Package for Parallel Computers*, version 4.6, Pacific Northwest National Laboratory: Richland, WA, 2004.
(30) Becke, A. D. *J. Chem. Phys.* **1990**, *98*, 5648−5652.
(31) Becke, A. D. *Phys. Rev. A* **1988**, *38*, 3098−3100.
(32) Perdew, J. P. *Phys. Rev. B* **1986**, *33*, 8822−8824.
(33) Schafer, A.; Horn, H.; Ahlrichs, R. *J. Chem. Phys.* **1992**, *97*, 2571−2577.
(34) *NBO 5.0*. Glendening, E. D.; Badenhoop, J. K.; Reed, A. E.; Carpenter, J. E.; Bohmann, J. A.; Morales, C. M.; Weinhold, F. Theoretical Chemistry Institute, University of Wisconsin: Madison, WI, 2001; http://www.chem-.wisc.edu/−nbo5.
(35) (a) Kahn, O. *Molecular Magnetism*; VCH Publishers: New York, 1993. (b) O'Connor, C. J. *Prog. Inorg. Chem.* **1982**, *29*, 203−283.
(36) James, F. *MINUIT*, version 94.1; CERN Program Library; CERN Geneva, Switzerland.

Acknowledgment. We are grateful to the Fonds der Chemischen Industrie, and the Göttinger Akademie der Wissenschaften for support of this work. FIRB and PRIN funds from Italian MIUR are gratefully acknowledged.

Supporting Information Available: Details of the single-crystal X-ray structure determination of **2** and **3** (CIF files). The temperature dependence of the magnetic susceptibility of **3** (Figure S1, PDF). The electronic spectra (EPR) of **2** (Figures S2a and S2b, PDF). This material is available free of charge via the Internet at http://pubs.acs.org.

JA042269E